ELSEVIER

Biochimica et Biophysica Acta 1310 (1996) 53–59

BBA Biochimica et Biophysica Acta

Retrovirus budding may constitute a port of entry for drug carriers

C. Ropert [a,*], Z. Mishal [b], Jr., J.M. Rodrigues [c], C. Malvy [a], P. Couvreur [c]

[a] *URA 147 CNRS, U 140 INSERM, Institut Gustave Roussy, Rue Camille Desmoulins, 94805 Villejuif cedex, France*
[b] *CNRS UPS 47, Laboratoire de cytométrie, Villejuif cedex, France*
[c] *URA CNRS 1218, Université PARIS XI, Centres d'Etudes Pharmaceutiques, 5 rue Jean Baptiste Clément, 92296 Chatenay-Malabry cedex, France*

Received 1 June 1995; accepted 9 August 1995

Abstract

This paper investigates the relation between viral infection and cell uptake of liposomes and nanoparticles. A defective virus was used to infect two types of cells: cells allowing virus budding (psi2*neo* cells) and cells bereft of a virus exit process (NIH 3T3 cells). This study has revealed that cell uptake of pH-sensitive-liposomes is highly dependent on the virus exit process, since it ensued only when virus budding occurred. This preferential uptake of pH-sensitive liposomes by infected cells was not carrier-specific because similar uptake was observed with non-biodegradable fluorescent nanoparticles using confocal microscopy. Also, inhibition of *neo* gene expression by oligonucleotide pH-sensitive-liposomes was only observed in the cell system (psi2*neo*) endowed with a virus exit process. Finally, increased membrane fluidity was noted in the infected cells, possibly reflecting membrane perturbation due to virus budding. We suggest that this membrane perturbation may be the key to the uptake of the different colloidal carriers. Infected cells could, thus, constitute a natural target for particulate drug carriers.

Keywords: Liposome; Nanoparticle; Retrovirus budding; pH sensitivity

1. Introduction

Since the discovery of the agent responsible for AIDS and the devastating effects of this virus, new antiretroviral therapies are urgently needed. Oligonucleotides are potential antiviral molecules capable of controlling viral gene or oncogene expression (see review, Hélène and Toulmé) [1]. They have been used successfully in cell culture to inhibit the expression of specific HIV genes [2–4] and there is now widespread interest in extending the use of antisense compounds to the in vivo setting [5,6]. Many chemical modifications have been proposed to solve the problem of the enzymatic degradation of the oligonucleotides (see review, Goodchild) [7]. 'Drug carrier systems' such as nanoparticles [8] and liposomes [9–11] have been used to enhance the cellular uptake of these compounds, of the duration of their activity and to target them more efficiently. A major drawback of carrier systems in treatment strategies is that they are not cell-specific. Liposomes, however, can be coupled to various ligands, such as monoclonal antibodies, which then permit their targeting of specific cell populations [9,12]. But the efficiency of this process is dependent on the nature of the targeted surface molecules and on the size of the liposome used [13,14]. Recently, oligonucleotides directed against the *env* mRNA of the murine Friend retrovirus were encapsulated in pH-sensitive liposomes and an antisense activity was noted with this type of carrier [15]. These liposomes are stable at physiological pH, but after being internalized by cells via an endocytic pathway, liposomes exposed to the acidic pH of the endosome are destabilized and possibly fuse with the endosome membrane. This results in the release of their contents into the cytoplasm without degradation by lysosomal enzymes. A slight difference of the activity has been observed between oligonucleotides encapsulated in pH-sensitive liposomes and non-pH-sensitive liposomes [16]. This finding prompted us to investigate interactions between cells and liposomes.

This paper is an attempt to identify the mechanism governing uptake of liposomes by infected cells. Two types of investigations have been performed. We first tried to determine the relationship between cellular uptake and activity of oligonucleotide liposomes and retrovirus budding. Secondly, using polystyrene nanoparticles (with roughly the same size as liposomes), we compared uptake

* Corresponding author. Fax: +33 3473 7816.

SSDI 0167-4889(95)00140-9

by infected and non-infected cells. The present study shows, for the first time, that in vitro cell uptake of colloidal carriers (liposomes or polystyrene nanoparticles), whatever their composition, is directly dependent on the process whereby the retrovirus exits from murine fibroblasts. This observation could stimulate new strategies in the treatment of retroviral infections.

2. Materials and methods

2.1. Oligonucleotide synthesis

The oligonucleotide target was the *neo* gene present in psi2*neo* cells and in transfected NIH 3T3 cells. The antisense complementary to the 5′ region of the initiation codon AUG of the *neo* gene was synthesized on an automated DNA synthesizer (model 380 B, Applied Biosystems, Foster City, CA, USA). The sequence was 5′GCGTACTAACTTGTT3′. The control oligomer had the following reverse antisense composition: 5′ TTGTTCAATCATGCG3′. The oligonucleotides were purified by ethanol precipitation and centrifugation. The 5' end of the oligonucleotides was labeled with ^{32}P using T4 polynucleotide kinase at 37°C for 30 min. The quality of oligonucleotide purification was then evaluated through electrophoresis (20% polyacrylamide 7 M urea gel).

2.2. Preparation of liposomes

Liposomes were prepared by reverse phase evaporation[15]. Briefly: the organic phase was constituted by ethanol/chloroform at a ratio of 1:1 in which phospholipids (phosphatidylethanolamine/acide oleic/cholesterol at a ratio of 10:5:2) were dissolved. The aqueous phase was composed of oligonucleotides at 600 μg/ml in a buffer (Tris EDTA, pH = 7.8). Non-encapsulated oligonucleotides were separated from liposomes by Sepharose 4B gel filtration. The liposomes were labelled with ^{14}C dioleylphosphatidylethanolamine (Amersham) and the activity used in the final preparation was 0.02 μCi/μmol of phospholipids.

2.3. Preparation of fluorescent polystyrene nanoparticles

Polystyrene nanoparticles were prepared using the method reported by Fessi et al. [17], which was slightly modified. Briefly, 10 mg of Polystyrene (Estapor®, Prolabo, France) and 5 mg of phospholipids (Epikuron® 170, Lucas Meyer) were dissolved in 10 ml of acetone; the solution was mixed, under magnetic stirring, with an aqueous phase (20 ml) containing 5 mg of Poloxamer® (ICI). After 10 min of stirring, acetone and water were evaporated under vacuum until a volume of 5 ml was reached. Particle size distribution, the average size and polydispersity index were measured by laser light scattering using a monochromatic laser ray diffusion counter (Nanosizer N4, Coultronics, Margency, France). The nanoparticles had a monodiperse size distribution of between 170 and 200 nm.

2.4. Cell lines and virus

The cells used were derived from the NIH 3T3 cells (murine fibroblasts). Psi2*neo* cells [18]: they were obtained by transfection of the SVX shuttle vector (defective virus devoid of three viral genes: *gag*, *pol*, *env*). These cells contained these three viral genes in their genome and therefore allowed the budding and exit of the defective virus. F57 were NIH 3T3 cells chronically infected by Friend retrovirus. All cell lines were growing in DMEM medium with 5% fetal bovine serum (heated at 56°C 30 min) and antibiotics.

Two types of virus were used: a shuttle vector (SVX); this is a defective virus devoid of three viral genes (*gag*, *pol*, *env*) with the *neo* gene encoding for resistance to geneticin. The other retrovirus used was the murine Friend retrovirus.

2.5. Selection of transfected cells by shuttle vectors

The selection of the transfected cells was based on the geneticin resistance assay described below. Only the cells transfected by the defective virus and therefore containing the *neo* gene were able to grow in the presence of geneticin. NIH 3T3 cells (3.10^5) were plated in 60-mm Petri dishes and incubated at 37°C. Twenty hours after incubation, the defective virus was added. Twenty hours following infection, geneticin was added at a concentration of 0.6 mg/ml. Six days later the resistant clones were then replaced to obtain an homogeneous population of NIH 3T3 having integrated the *neo* gene (no virus budding occurred in these cells).

2.6. Detection of antisense activity of oligonucleotides directed against the neo gene

In order to evaluate the impact of virus budding on the efficiency of the encapsulated oligonucleotides, the *neo* gene was chosen as the target since it was present in psi2*neo* cells and in transfected NIH 3T3. Psi2*neo* cells (3.10^5/plate) were incubated with oligonucleotides, free or encapsulated in pH-sensitive liposomes at different concentrations or with empty liposomes. The anti-*neo* activity was estimated using the resistance to geneticin assay. In the case of these chronically transfected cells, the operating conditions were as follows: 24 h after the addition of encapsulated or free oligonucleotides or empty liposomes to the psi2*neo* cells, the culture medium containing the defective virus was removed and used for the transfection of NIH 3T3 after appropriate dilution (in order to obtain 150 clones). Selection of cells having integrated the *neo* gene was then performed: 20 h after the infection, geneticin was added at a concentration of O.6 mg/ml. Six

days later the resistant clones were stained using crystal violet dye and counted. We verified that the number of defective viruses introduced was proportional to the number of resistant clones obtained. In a parallel experiment the transfected NIH 3T3 cells (3.10^5/plate) were incubated with free or encapsulated oligonucleotides or empty liposomes, followed 24 h later, by selection with geneticin.

2.7. Uptake of oligonucleotide-liposomes

Oligonucleotide-^{14}C DOPE liposomes were added to fibroblasts (3.10^5/plate). The final concentration of oligonucleotides in the culture medium was 0.32 μM and 0.3 mM for the phospholipids. Cells were pelleted, washed three times in phosphate-buffered saline and the successive supernatants were pooled. Then the cells were lysed by adding water. The cell fraction was centrifuged at 10000 $\times g$ for 5 min, leading to a pellet containing the nucleus and the membranes, whereas the supernatant corresponded to the cytoplasmic fraction supernatant. The three fractions (extracellular medium, cytoplasm and membrane pellet) were counted to evaluate oligonucleotide uptake and its association with the membrane fraction.

2.8. Confocal microscopy

Cells (NIH 3T3 and chronically infected F_{57} cells) were incubated with fluorescent polystyrene nanoparticles (100 μl/dish) for 24 h. Confocal microscopy was then carried out, directly, on the cells in the Petri dishes. The interactive confocal scanning laser microscope used was the ACA 570 (MERIDIAN Instruments Okemos MI) with a laser power of 20 Mw and a neutral density filter (10% transmission). The fluorescent images were obtained with an excitation wavelength of 457 nm, close to the maximum excitation of the fluorescent polystyrene; the emission was observed using a band-pass filter at 500 nm. The scans were acquired on sections of 1 μm of the cells.

2.9. Fluorescence polarization studies

The fluorescent membrane probe, 1.5 diphenyl-1.3.5-hexatriene (DPH), was purchased from Sigma. Two mmoles of DPH in tetrahydrofuran were added into 100 ml of PBS (pH 7.4), giving a final DPH concentration of 2 mM [19]. A total of 10^6 NIH 3T3 or F57 cells were incubated with DPH for 30 min at 25°C. Then the cells were analysed on a FACS-440 (Becton and Dickinson, USA) cell sorter. The instrument analyzed the cells in aqueous suspension as they passed through an argon ion laser at 363 nm. Dead cells were excluded by light scatter gating measurements. The degree of fluorescence polarization (P) was calculated by simultaneous detection of apparent fluorescence intensity in planes parallel and perpendicular, respectively, to the polarization plane of exciting light [20]. The on-line computer calculated the fluorescent polarization for each cell according to the following Eq. (1): $(I_\perp - I_\parallel)/(I_\perp + I_\parallel)$, where $I_\parallel$ and $I_\perp$ were the fluorescence intensity values recorded when fluorescent light passed through polarizers, oriented parallel and perpendicular, respectively, to the polarized excitation light. P-values were reflected membrane packing. The steady-state fluorescence anisotropy (r_s) values were calculated from the P-values that could be deduced from Eq. (2). The determination of the order parameter S was performed from r_s using Eq. (3). These parameters do not provide information on membrane viscosity directly, but rather on membrane packing.

$$r_s = (I_\parallel - I_\perp)/(2I_\parallel + I_\perp) \quad (2)$$

$$S = \frac{[1 - 2r_s/0.4 + 5(r_s/0.4)2]1/2 - 1 + r_s/0.4}{r_s/0.4} \quad (3)$$

3. Results

3.1. Inhibition of neo gene expression

Oligonucleotide liposomes were added to psi2*neo* cells (transfected cells, which produced recombinant virus containing the *neo* gene) and anti-*neo* activity was measured and expressed as the percentage of inhibition of resistant clones growing with geniticin (Table 1). In these conditions significant inhibition of *neo* gene expression was observed which corresponded to a decrease in the produc-

Table 1
Inhibition of *neo* gene expression in cells by oligonucleotides encapsulated in pH-sensitive liposomes

		% of inhibition of growth of geneticin-resistant clones			
		Oligonucleotide concentration (μM)			
		0.08	0.12	0.16	0.24
Antisense oligo	psi2neo	22 ± 4	54 ± 6	70 ± 6	82 ± 8
	3T3 infected	7 ± 2	6 ± 1	12 ± 2	11 ± 3
Control oligo	psi2eo	4 ± 1	3 ± 1	5 ± 2	8 ± 3
	3T3 infected	5 ± 2	7 ± 1	8 ± 3	9 ± 3

The values are expressed as the percentage of inhibition of the growth of geneticin-resistant clones. The anti *neo* oligonucleotides, encapsulated in pH-sensitive liposomes, were added to cells containing the *neo* gene (3T3 and psi2*neo* cells). After 24 h, a selection was performed with geneticin. The values are expressed as the percentage of inhibition of the growth of geneticin resistant clones. The values are the mean of two experiments.

tion of defective viral particles containing the *neo* gene. This inhibition was measured after secondary infection of the recipient cells. The IC_{50} of liposomes with antisense oligonucleotides was evaluated as 0.12 μM, whereas free oligonucleotides were unable to inhibit *neo* gene expression up to a concentration of 25 μM. No activity was detected for control oligonucleotide liposomes (Table 1). The addition of either oligonucleotide liposomes, or free oligonucleotides had no effect on *neo* gene expression, whatever the concentrations, in NIH 3T3 cells (selected to contain the *neo* gene after transfection by the defective virus). Empty liposomes had no effect on the inhibition of *neo* gene expression in either cell line (psi2*neo* and 3T3 cells).

3.2. Uptake of oligonucleotide liposomes by 3T3 or psi2neo cells

In order to determine whether virus exiting affected the uptake of ^{14}C DOPE liposomes, radioactivity was measured in the three cell fractions (cytoplasm, the membrane pellet and supernatant) of SVX-infected cells (NIH 3T3 cells and of psi2*neo*). As shown in Table 2, the bulk of the radioactivity was confined to the membranes of non-infected NIH 3T3 cells. The same result (absence of uptake) was observed for the NIH 3T3 cells infected by the defective virus; it is noteworthy that the exit of the virus did not occur in this cell line. Only a small amount of radioactivity was detected in the cytoplasm. On the contrary, with the psi2*neo* cells, in which the exit of the virus occurred, a significant amount of radioactivity was found in the cytoplasm. It is noteworthy that although a significant amount of radioactivity was found in the membrane of all the cells after 6 h of incubation, it was only found in the cytoplasm of the psi2*neo* cells.

Table 3
Values of fluorescent polarisation (P), fluorescence emission anisotropy (r_s) and order parameter (S) of Friend-infected and non-infected fibroblasts

	P	r	S
Non-infected cells	0.278 ± 0.003	0.200 ± 0.003	0.648 ± 0.009
Infected cells	0.257 ± 0.004	0.187 ± 0.004	0.581 ± 0.012

The cells (10^6/plate) were incubated with a fluorescent membrane probe (DPH) and the suspension was analyzed on a FACS-440. The degree of fluorescent polarization was calculated by simultaneous detection of apparent fluorescence intensity in planes parallel and perpendicular to the polarization plane of the exciting light (the values of r and S were deduced from P). The data are the mean of three experiments.

3.3. Confocal microscopy

In order to evaluate the presence of the carrier in infected and non-infected fibroblasts, a study with fluorescent nanoparticles was undertaken using confocal microscopy. The cell system used was F57 cells chronically infected by the friend retrovirus. We have previously explored this system and demonstrated the efficiency of oligonucleotides encapsulated in pH-sensitive liposomes.

The violet colour in all the figures corresponds to background autofluorescence intensity according to the fluorescence scale. Fig. 1a represents different sections of non-infected cells after incubation with fluorescent nanoparticles. The fluorescence was mainly located in the first sections, corresponding to the cell membrane (blue spot in section 4 to section 6); in the following sections, the fluorescence has disappeared. As indicated, sections 8-9 correspond to the larger section of the cell. On the contrary, after incubation of the fluorescent nanoparticles with the infected cells, the bulk of the fluorescence was located in the slices corresponding to the cell interior. A

Table 2
Distribution kinetics of oligonucleotide ^{14}C liposomes in transfected and non-transfected cells

	h	3T3 cells	3T3-transfected cells	Psi2 neo cells
% in cytoplasmic fraction	6	0.1	0.2	5.3
	18	0.3	0.3	7.7
	24	0.5	1.0	11.4
	36	1.1	1.5	17.5
	48	1.5	2.7	21.3
% in the membrane pellet	6	4.5	5.7	9.3
	18	6.2	7.8	12.1
	24	8.5	11.3	14.2
	36	13.5	18.6	23.5
	48	19.8	24.2	25.4
% non-cell-associated	6	95.4	94.1	85.4
	18	93.5	91.9	80.2
	24	91.0	87.7	74.4
	36	85.4	79.9	59.0
	48	78.7	73.1	53.3

Cells were plated and incubated with the oligonucleotide ^{14}C DOPE liposomes (0.3 mM of phospholipids), the cells were lysed by adding water and the three fractions (medium, cytoplasm and membranes) obtained by centrifugation. Radioactivity was counted to evaluate the distribution of liposomes in the different fractions ($n = 2$).

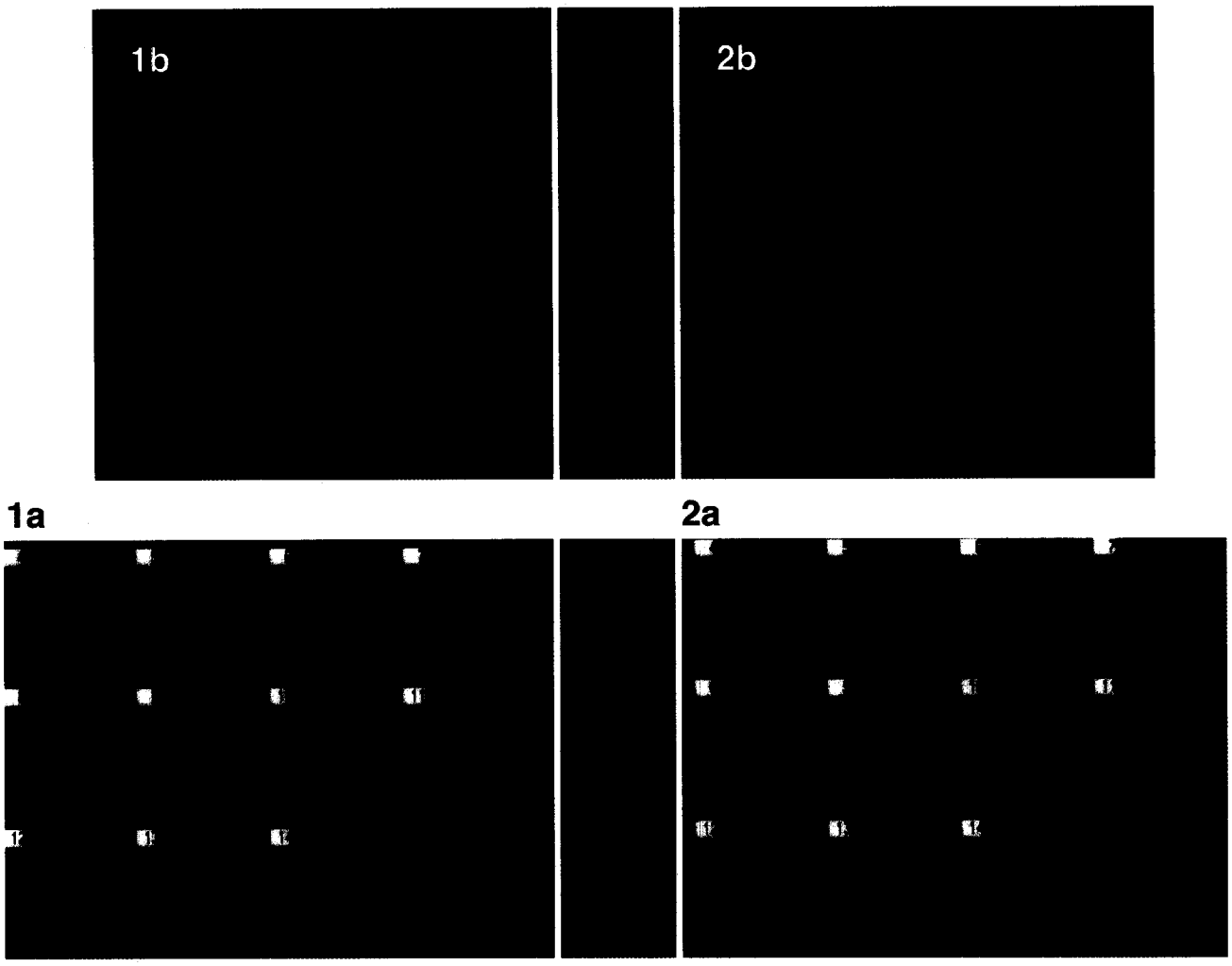

Fig. 1. (a) Uptake of the fluorescent nanoparticles by non-infected fibroblasts in confocal microscopy at 37°C. Different images of fluorescence at 1 μm increments along the Z-axis of cells. Sections 9–10 correspond to the larger section of the fibroblasts. (b) A 3-D reconstruction of 16 sections scanned at 1-μm increments along the Z-axis of the non-infected cells labelled with fluorescent nanoparticles.

Fig. 2. (a) Uptake of the fluorescent nanoparticles by chronically infected fibroblasts in confocal microscopy at 37°C. Different images of fluorescence at 1-μm increments along the Z-axis of cells. Sections 9–10 correspond to the larger section of the fibroblasts. (b) A 3-D reconstruction of 16 sections scanned at 1-μm increments along the Z-axis of the chronically infected cells labelled with fluorescent nanoparticles.

blue spot appeared in section 6 and fluorescence intensification was observed in sections 8-9-10 (Fig. 2a). When the fluorescent images of the individual sections were summed to reconstitute the fluorescence emitted by the entire cell, the fluorescence was found to be located in the heart of cell for infected cells (Fig. 2b), and limited to the cell membrane for non-infected cells (Fig. 1b).

3.4. Fluorescence polarization

Fluorescent polarization of DPH-labelled cells has been previously shown to reflect changes induced by DMSO in the membrane properties of Friend leukaemic cells [19]. As DPH proved to be a sensitive marker for labelling fluorescent polarization study, we chose to investigate the fluorescence polarization (P) of infected and non-infected murine fibroblasts with this method in this study. As shown in Table 3, P-values were significantly decreased in infected cells, this being related to the microviscosity of the cell membrane. This signifies that membrane fluidity was greatly affected in infected cells compared to that in non-infected ones.

4. Discussion

In a previous work [16], we demonstrated the dramatic impact of viral infection on liposome penetration into cells [16]. With a system combining the exit of defective virus (psi2*neo* cells containing *gag*, *pol*, *env* viral genes) and

cells bereft of this exit process (transfected NIH 3T3), we have attempted to describe the mechanism of liposome uptake by infected cells. In fact such a system allowed us to appreciate the impact of virus budding on oligonucleotide liposome uptake. Indeed, in cells allowing virus budding (psi2neo), oligonucleotide liposomes were detected in the cytoplasm, whereas with transfected NIH 3T3 cells (devoid of an exit for viral particles) most of the radioactivity was confined to the cell membrane. These results provide compelling evidence that cellular uptake of liposomes is strongly correlated with virus budding. A striking difference was noted between the activity of encapsulated oligonucleotides in the two cell lines (psi2neo and 3T3). Clearly, the inhibition of *neo* gene expression by oligonucleotide liposomes was only observed in cells with a virus exit process. This inhibitory activity can therefore be correlated with uptake of oligonucleotide liposomes by these cells. It also suggests that oligonucleotide liposome efficacy is contingent on the intracellular delivery of the oligomers.

In order to confirm the preferential uptake of the liposomes by infected cells allowing virus budding, the fate of fluorescent polystyrene nanoparticles in infected and uninfected cells was investigated using confocal microscopy. The non-biodegradability of the polystyrene nanoparticles is of major interest when assessing whether fluorescence localization unequivocally corresponds to nanoparticles. This experiment revealed that, like liposomes, nanoparticles were selectively taken up by the infected cells. Thus, the preferential capture of colloidal carriers by infected cells seemed to be totally unrelated to the nature of the carrier (liposomes or nanoparticles) and only dependent on the state of the cells (infected with virus budding or not).

The difference in the capture of liposomes or nanoparticles observed between infected and non-infected cells could be explained by the effect the virus exerts on the host cell membrane. The viral envelope is in fact composed of a bilayered lipid derived from the cell membrane. It is noteworthy that a variation in membrane fluidity of HIV infected cells has been observed, resulting, according to certain authors [21], in an increase in membrane fluidity, whereas others [22] have observed a decrease in membrane fluidity as deduced from lipid composition.

We directly investigated membrane fluidity of the infected and uninfected fibroblasts by measuring fluorescence polarization. The P-values measured (polarization values related to the microviscosity of the cell membranes) suggested that the increase in membrane fluidity was of a greater magnitude in infected cells. This increase probably reflects certain modifications in the dynamic process of the cell membrane triggered by virus budding which may be assimilated with an exocytosis process. In several cell systems, exocytosis is followed by the activation of pinocytosis [23–25]. This may result from the recapture and a re-use of the vesicle membrane, so that the overall dimensions of the cells and of the vacuolar system remain constant [26]. For these reasons virus budding may stimulate fibroblast pinocytic activity and thus explain the increased cell capture of particulate drug carriers.

That the virus budding is required for cell internalization of liposomes may prove essential for the development of new drug targeting strategies. However, further investigations are needed with other viruses and cells to determine whether this is a general phenomenon or not among non-professional phagocytes.

Acknowledgements

We thank Dr. F. Subra for his precious help, notably concerning the psi2*neo*. system. We thank Dr. E. Lescot for the synthesis of phosphodiester oligonucleotides. This research was supported by grants from the Agence Nationale de Recherche sur le SIDA, INSERM and CNRS. J.M.R.Jr. received a fellowship from CAPES (Brazil). The authors are grateful to L. St Ange for the linguistic revision of the manuscript.

References

[1] Helene, C. and Toulmé, J.J. (1990) Biochim. Biophys. Acta 1049, 99–125.
[2] Agrawal, S., Ikeuchi, T., Sun, D., Sarin, P.S., Konopka, A., Maizel, T. and Zamecnick, P.C. (1988) Proc. Natl. Acad. Sci. USA 86, 7790–7794.
[3] Goodchild, J., Agrawal, S., Civeira, M.P., Sarin, P.S., Sun, D. and Zamecnik, P.C. (1988) Proc. Natl. Acad. Sci. USA 85, 5507–5511.
[4] Lisziewicz, J., Sun, D., Metelev, V., Zamecnick, P.C., Gallo, R.C. and Agrawal, S. (1993) Proc. Natl. Acad. Sci USA 90, 3860–3864.
[5] Akthar, S. and Juliano, R.L. (1991) Pharm. J. 247, 89–92.
[6] Cohen, J.S. (1989) Trends Pharmacol. Sci. 10, 435–437.
[7] Goodchild, J. (1990) Bioconj. Chem. 11, 165–187.
[8] Chavany C., Le doan, T., Couvreur, P., Puisieux, F. and Hélène, C. (1992) Pharm. Res. 9, 441–449.
[9] Leonetti, J.P., Machy, P., Degols, G., Lebleu, B. and Leserman, L. (1990) Proc. Natl. Acad. Sci. USA 87, 2448–2451.
[10] Zelphati, O., Zon, G. and Leserman, L. (1993) Antisense Res. Dev. 3, 323–338.
[11] Thierry, A.R. and Dritschilo, A. (1992) Nucleic Acid Res. 20, 5691–5698.
[12] Milhaud, P.G., Machy, P., Lebleu, B. and Leserman, L. (1989) Biochim. Biophys. Acta 987, 15–20.
[13] Machy, P. and Leserman, L. (1983) Biochim. Biophys. Acta 730, 313–320.
[14] Matthay, K.K., Abai, A.M., Cobb, S., Hong, K., Papahadjopoulos, D. and Straubinger, R.M. (1989) Cancer Res. 49, 4879–4886.
[15] Ropert, C., Lavignon, M., Dubernet, C., Couvreur, P. and Malvy, C. (1992) Biochem. Biophys. Res. Comm. 183, 879–885.
[16] Ropert, C., Malvy, C. and Couvreur, P. (1993) Pharm. Res. 10, 1427–1433.
[17] Fessi, H., Puisieux, F., Devissaguet, J.-P. Ammoury, N., Benita, S. (1989) Int. J. Pharm. 55, R1–R4.
[18] Subra, F., Mouscadet, J.F., Lavignon, M., Roy, C. and Auclair, C. (1993) Biochem. Pharm. 45, 93–99.
[19] Mishal, Z., Fourcade, A. and Tapiero, H. (1981) Cytometry 2, 165–169.

[20] Shinitzky, M. (1984) in Physiology of Membrane Fluidity, Vol. I, pp. 1–57, CRC Press, Boca Raton, FL.
[21] Aguilar, J.J., Anel, A., Torres, J.M., Semmel, M. and Uriel, J. (1991) AIDS Res. and Human Retroviruses 7, 761–765.
[22] Apostolov, K., Barker, W., Galpin, S.A., Habib, N.A., Wood, C.B. and Kinchington, D. (1989) FEBS Lett. 250, 241–244.
[23] Holtzman, E., Freeman, A.R. and Cashner, A. (1971) Science 173, 733–736.
[24] Cecarelli, B., Huribut, W.P and Mauro, A. (1972) J. Cell. Biol. 23, 85–94.
[25] Heuser, J.E. and Reese, T.S. (1973) J. Cell. Biol. 57, 315–344.
[26] Steiman, R.M., Mellman, I.S., Muller, W.A. and Cohn, Z.A. (1983) J. Cell. Biol. 96, 1–27.